X-ray Single Photon 1-D Imaging Spectrometers

L. Li, L. Frunzio, C. Wilson, K. Segall and D.E. Prober
A.E. Szymkowiak and S.H. Moseley

Abstract— **We have developed superconducting single-photon 1-D imaging x-ray detectors with an energy resolution of 13 eV FWHM at 6 keV and 1-D spatial resolution of 0.25 μm over a length of 20 μm in an effective area of 20 × 100 μm^2. The energy resolution along the 200 μm long absorber is 36 eV. The energy resolution of 13 eV is among the best reported for this kind of detectors and is within factor of 2 of its theoretical limit. The signals are read out by low-noise current amplifier with a dc voltage bias. The electronic noise measured by injecting pulses is 8 eV FWHM at 6 keV. By cooling the feedback resistor the current noise is reduced from 160 fA/Hz$^{1/2}$ to 90 fA/Hz$^{1/2}$.**

Index Terms— **imaging, single photon, spectrometer, superconducting tunnel junction, x-ray detector**

I. Introduction

Superconducting tunnel junction detectors (STJs) have been intensively studied in last decade as non-dispersive, single photon spectrometers for the energy range from 1 eV to 10 keV [1-5], because of their predicted high energy resolving power, E/ΔE. This good energy resolution arises from the much lower energy, ~meV, necessary to create a quasiparticle compared to the electron-hole pair excitation energy in a conventional semiconductor detector. The STJ can be used in astronomical observations, material analysis and other spectroscopy applications. The STJ also provides photon timing information with high quantum efficiency.

When a photon is absorbed in an STJ detector, it breaks Cooper pairs and creates excess quasiparticles, the number of which is

$$N_0(E) = \frac{E}{\varepsilon} \pm \sqrt{\frac{E}{\varepsilon} F}$$

where E is the incident photon energy, ε =1.74 Δ (2Δ is the energy gap of a superconductor absorber) is the effective energy required to create a single excitation (quasiparticle) and F is the Fano factor. We assume F=0.22 [6]. The ideal energy resolution of the STJ detector due to the creation statistics of the single-electron excitations is ΔE=2.355 $(F\varepsilon E)^{1/2}$, which gives 2.96 eV Full-Width-at-Half-Maximum (FWHM) at 5.9 keV for Ta absorber. However, for the device with significant backtunneling, the effective F is about 1.3 [7,8].

Manuscript received September 17, 2000.

Liqun Li, L. Frunzio, C. Wilson, K. Segall and D.E. Prober are with the Department of Applied Physics and Physics, Yale University, New Haven, CT 06520 USA (telephone: 203-432-4280, e-mail: daniel.prober@yale.edu).

A.E. Szymkowiak and S.H. Moseley are with NASA Goddard Space Flight Center.

II. Device Geometry and Experimental Setup

We have developed Ta-Al-AlOx-Al tunnel junction detectors for astrophysical application. The device uses a lateral double junction geometry, which can implement 1-D spatial imaging with only two readout channels. The 2-junction device geometry is shown in Fig. 1.

A photon is absorbed in the Ta film and the resulting quasiparticles cool rapidly to the Ta energy gap (Δ_{Ta}=700 μeV). They then diffuse to the two Al traps, where they enter at an energy Δ_{Ta}, cool toward the Al gap (Δ_{Al}=180 μeV) and are trapped in the Al by phonon emission, and then they tunnel. The ratio of charge collected in the two traps gives a measure of the position of the photon absorption. The sum of the charges provides information on the photon energy.

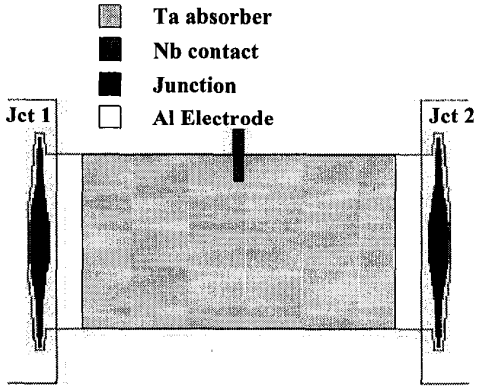

Fig. 1. Device geometry of a 1-D imaging STJ detector using lateral trapping.

The 1-D imaging STJ detector we measured has a 570 nm thick, 100 × 200 μm^2 Ta absorber. A 5 μm thin strip of niobium (Δ_{Nb}=1.5 meV) makes electrical contact to the center of the absorber, in order to prevent diffusion of the quasiparticles from the lower gap Ta into the higher gap Nb contact. There is an Al-AlOx-Al junction on each side of the Ta absorber with 10 μm overlap between Al and Ta. The thickness of bottom and top Al layer of the junctions is 210 and 445 nm, respectively. The junction area is 460 μm^2. Our tantalum film has RRR (residual resistance ratio) of 17. The

AlOx barrier has an estimated thickness of about 1 nm. Each Al junction has a normal state resistance of 1.4 Ω. The subgap current is 6 nA at a base temperature of 220 mK with a bias voltage 120 μV.

The device has been tested in a 2-stage ^{3}He cryostat at its base temperature of 220 mK. The magnetic field, about 20 Gauss, is applied in the plane of the junctions, perpendicular to the long (112 μm) edge of the junction, to suppress the DC Josephson current for stable DC biasing and to reduce the current at the Fiske mode at 160 μV. The quiescent dynamic resistance at a bias voltage of 120 μV is 50 kΩ. The device is illuminated with an ^{55}Fe x-ray source which emits the Mn K_α (E=5895 eV) and Mn K_β (E=6490 eV). The Mn K_α line is composed of 2-lines whose centers are separated by 11 eV. The absorption efficiency of our Ta absorber is 28%. The feedback resistors are cooled to reduce the Johnson noise. The preamplifier has a current noise of 90 fA/Hz$^{1/2}$, a voltage noise of 0.5 nV/Hz$^{1/2}$ and bandwidth of 100 kHz [9]. The amplified x-ray pulses are digitized by a Nicolet Integra 40 Oscilloscope. The digitized pulses are acquired by a computer. We apply various digital filters to the current pulses to obtain the best energy resolution. The charge is calculated by integrating of the current signal. The total electronic noise of the STJ in its quiescent state (without x-ray) and the amplifier can be measured using injected current pulses.

III. Experimental Results

Fig. 2 shows a plot of the two detector charge outputs Q_1 vs. Q_2, filtered with a fifth order 4 to 90 kHz Chebyshev filter. The filter reduces the total charge by a factor of three but maximizes the signal-to-noise ratio. With no quasiparticle loss in the absorber the Q_1 vs. Q_2 plot should be a straight line for a fixed photon energy. The lifetime of quasiparticles in the Ta absorber is long, and the curvature in the plot is actually due to the filtering of the pulses with different shapes from different locations.

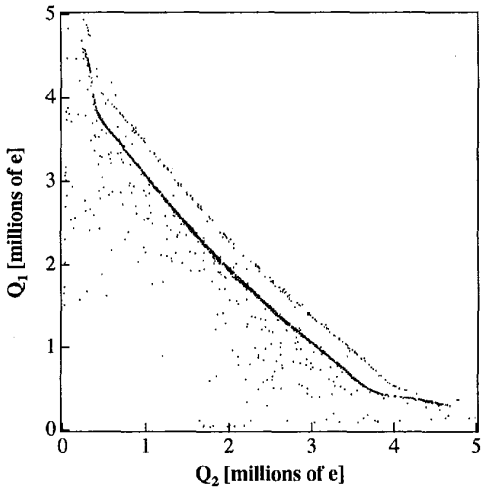

Fig. 2. Charge collected in junction 1 vs. charge collected in junction 2. The data has been filtered.

Because of the overlap between the Ta and Al, the device has an active area of 180 × 100 μm^2. A photon absorbed in the overlap region sees a reduced Ta gap, and thus produces more charge. This explains the upturn of the Q_1 vs. Q_2 plot at each end. Also, the "hotspot" just after absorption is ~ 10 μm wide, so the useful length of the absorber is ~ 160 μm. The lifetime of quasiparticles in the Ta is long, about 450 μs, so the absorber could be longer and thicker to improve the effective area and absorption efficiency. The measured energy resolution along the full absorber is 36 eV FWHM. In the selected range of 20×100 μm^2 at one side of the absorber the energy resolution is 13 eV for individual Mn $K_{\alpha1}$ and $K_{\alpha2}$ lines. The performance of the device is among the best for STJ detectors. The x-ray spectrum is shown in Fig. 3.

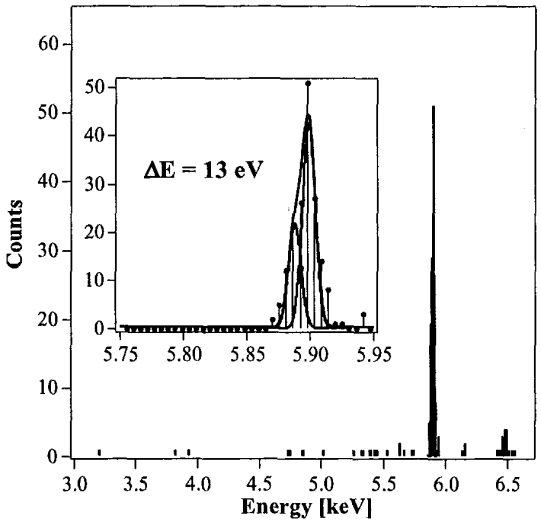

Fig. 3. The energy spectrum over a 20×100 μm^2 range of Ta absorber illuminated with an ^{55}Fe source. The inset shows amplification of the Mn K_α line and double peak fit of $K_{\alpha1}$ and $K_{\alpha2}$.

The advantage of this kind of device is that it can achieve high energy and spatial resolution. From the energy resolution we measured, we calculate the spatial resolution of the device [10]. In the selected region with energy resolution of 13 eV, the calculated spatial resolution is 0.25 μm. For the energy resolution of 36 eV at 5.9 keV along the whole absorber, the spatial resolution is 0.5 μm in 160 μm, equivalent to about 320 pixels along the length, with only two readout channels.

The quiescent electronic noise (without x-ray) is mainly due to the Johnson noise from the feedback resistor and shot noise of the device. By cooling the feedback resistor, we reduce Johnson current noise of the 1MΩ resistor from 130 fA/Hz$^{1/2}$ at room temperature to 10 fA/Hz$^{1/2}$ at about 1.5 K. Fig. 4 shows the measured current noise at the input with warm feedback resistor and cold feedback resistor. The ΔE of the injected electronic pulses is 11 eV with a warm feedback resistor, and it is 8 eV with a cold feedback resistor. To make further improvement in the future, a lower device temperature should be used to reduce the shot noise and

thermal quasiparticle loss in the junctions.

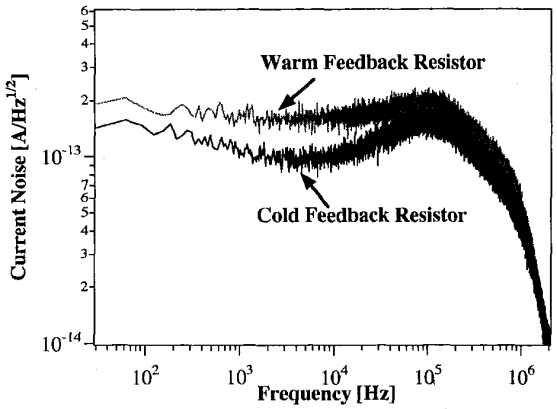

Fig. 4. Measured equivalent current noise at input with warm feedback resistor at room temperature compared to the one with cold feedback resistor at 1.5 K. The noise at 10 kHz is quoted.

A feature that affects the energy resolution specifically near the middle of the absorber is the Nb contact. Fig. 5 shows the total charge after filtering as a function of position. We clearly find that there is extra energy broadening in the middle of the device. This is order of 45 eV FWHM. We believe the extra energy broadening is due to the loss in the niobium lead or reduction of Δ_{Ta} proximitized by niobium. This problem might be solved by making a tantalum contact to the Al trap of one junction instead of a Nb contact to the center of the absorber.

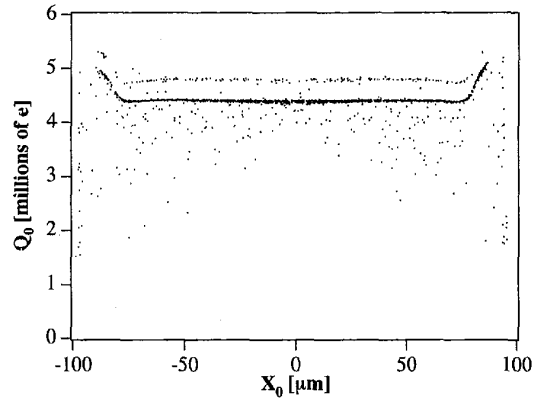

Fig. 5. Total charge vs. absorption location, corrected for loss.

This present device increases the energy resolving power a factor of two compared to the previous best device in our lab [5]. The improvement is due to a longer tunneling time (smaller junction area), which leads to better quasiparticle cooling prior to tunneling. It also allows us to bias the junction at a higher voltage to reduce the cancellation noise [11]. The subgap current is smaller, because the area is smaller, so the shot noise is smaller. However, this device also shows some small effects of self-recombination. The ratio of Mn K_β line to Mn K_α line is 1.09 instead of 1.10. It will not be a problem for lower energy x-ray photons. The energy resolution of 13 eV FWHM is computed after we consider this slightly nonlinear response. To avoid this problem we need to have the Al trap volume somewhat larger, and cool the device to lower temperature to further reduce the shot noise and thermal quasiparticle loss.

IV. Summary

In summary, we demonstrated single-photon imaging STJ detectors with an energy resolution of 13 eV FWHM in a $20\times100\ \mu m^2$ area, and 36 eV FWHM along the whole Ta absorber. The spatial resolution is about 0.5 μm in 160 μm. By using a cold feedback resistor the current noise reduces from 160 $fA/Hz^{1/2}$ to 90 $fA/Hz^{1/2}$. The electronic noise has been improved from 11 eV with warm feedback resistor to 8eV with cold feedback resistor. Cooling the device down to 0.1K can reduce the shot noise and thermal quasiparticle loss in the junctions and improve the energy resolution even further.

References

[1] N. Booth and D.J. Goldie, "Superconducting particle detectors", Supercond. Sci. Technol., vol. 9, pp.493-516, 1996.

[2] P.Verhoeve, N. Rando, A. Peacock, A. van Dordrecht, B.G. Taylor , and D.J.Goldie, "High-resolution x-ray spectra measured using tantalum superconducting tunnel junctions ", Appl. Phys. Lett., vol. 72, pp.3359-3361, 1998; J.B. le Grand et al., "A superconducting tunnel junction x-ray detector with performance limited by statistical effects ", Appl. Phys. Lett., vol. 73, pp. 1295-1297 ,1998.

[3] S. Friedrich et al., "Experimental quasiparticle dynamics in a superconducting, imaging x-ray spectrometer" Appl. Phys. Lett., vol. 71, pp.3901-3903, 1997.

[4] P. Hettl et al., "High resolution x-ray spectroscopy with superconducting tunnel junctions", Proc. EDXRF'98, Bologna, 7-12 June 1998.

[5] K. Segall et al., "Single photon imaging x-ray Spectrometers", IEEE Trans. Appl. Supercond., vol. 9, pp.3226-3229, 1999.

[6] Fano factor for Sn: M. Kurakado, "Possibility of high resolution detectors using superconducting tunnel junctions", Nucl. Instrun. Methods 196, pp. 275-277 (1982); for Nb: N. Rando et al., "The properties of niobium superconducting tunneling junctions as x-ray detector", Nucl. Instum. Methods Phys. Res. A 313, pp. 173-195, 1992. We assume Ta to be similar to Nb.

[7] D. J. Goldie, P.L. Brink, C. Patel, N.E. Booth, and G.L. Salmon, "Statistical noise due to tunneling in superconducting tunnel junction detectors", Appl. Phys. Lett., vol. 64, pp. 3169-3171, 1994.

[8] C.A. Mears, S.E. Labov, and A.T. Barfknecht, "Energy-resolving superconducting x-ray detectors with charge amplification due to multiple quasiparticle tunneling", Appl. Phys. Lett., vol. 63, pp. 2961-2963, 1993.

[9] S. Friedrich et al., "Single photon imaging x-ray spectrometers using low noise current preamplifiers with dc voltage bias", IEEE Trans. Appl. Supercond., vol. 3, pp. 3383-3386, 1997.

[10] H. Kraus et al., "Quasiparticle trapping in a superconductive detector system exhibiting high energy and position resolution", Phys. Lett. B, vol. 231, pp.195-202, 1989.

[11] K. Segall et al., "Noise mechanism in single photon, superconducting tunnel junction detectors", Appl. Phys. Lett. , vol. 76, pp. 3998-4000, 2000.